

Spatially Resolved Visible Luminescence of Self-Assembled Semiconductor Quantum Dots

R. Leon,* P. M. Petroff, D. Leonard, S. Fafard†

Ensembles of defect-free InAlAs islands of ultrasmall dimensions embedded in AlGaAs have been grown by molecular beam epitaxy. Cathodoluminescence was used to directly image the spatial distribution of the quantum dots by mapping their luminescence and to spectrally resolve very sharp peaks from small groups of dots, thus providing experimental verification for the discrete density of states in a zero-dimensional quantum structure. Visible luminescence is produced by different nominal compositions of $\text{In}_x\text{Al}_{(1-x)}\text{As}-\text{Al}_y\text{Ga}_{(1-y)}\text{As}$.

By virtue of its size and potential energy distribution, a semiconductor quantum dot (QD) structure confines carriers in three dimensions, allowing zero dimensions in their degrees of freedom and creating atom-like levels with discrete densities of states. Dimensions on the order of the localization of the electron (hole) wave function can be accomplished with a very small volume (1) of a material with a low band gap embedded in a material or materials with a larger band gap, allowing for a three-dimensional (3D) confinement potential for the electrons and the holes in the semiconductor with the lower band gap.

Compared to the growth of its 2D counterpart, the quantum well, QD fabrication represents an additional level of difficulty. Confinement for 0D and 1D structures in the past have made use of electron beam lithography techniques, which present problems. Quantum size dimensions are usually beyond the limit of standard lithography (features >0.1 μm), but even if this can be overcome by design ingenuity (2), interfacial impurities and surface damage, which can occur during processing, limit the performance of these quantum structures.

One of the recent promising advances in the fabrication of these devices that avoids most of these technological problems exploits one of the natural consequences in the growth modes for dissimilar materials. Various growth modes are possible in heteroepitaxy. The prevalence of one type of growth over the others de-

pends on the differences between crystal structures, the amount of strain or lattice mismatch, and the interfacial energies. The morphology of the growth can be layer-by-layer (3), island growth (4), or initial layer growth followed by island formation (5). The layer-by-layer growth mode is observed for lattice-matched materials of identical crystal structure, such as Au on Ag, or AlGaAs on GaAs. Direct island growth is seen in materials with a high interfacial energy. The third type of growth has been observed for crystals of dissimilar lattice spacing but low interfacial energy, like Ge on Si (6) or InAs on GaAs (7–14). In this process, the growth starts two dimensionally, as in the layer-by-layer mode, but after a certain thickness is reached, islands form spontaneously, and a thin 2D wetting layer is left under the islands. If the growth is allowed to continue beyond the initial island formation stage, misfit dislocations start forming at the island edges (15, 16), and these grow and coalesce. This is generally considered to be a most unfavorable growth situation.

It has recently been shown that QDs (17, 18) can be obtained with dislocation-free self-assembled coherent islands spontaneously formed from strained InAs grown directly on GaAs. In this process, the growth is interrupted immediately after the formation of the islands but before the islands reach a size for which strain relaxation and misfit dislocations occur. A uniform size distribution can be obtained at the early stages of the growth, producing island quantum-size islands. The spontaneous island formation during growth precludes the interface quality problems often associated with *ex situ* processed quantum structures of low dimensionality. This breakthrough in the fabrication of defect-free 0D structures provides the opportunity for experimental verification of the effects of 3D quantum confinement in semiconductor structures. Evidence for a discrete density of states can be seen from resonantly excited luminescence (19), magnetocapacitance measurements (20, 21), and emission of extra-sharp photolu-

minescence (PL) lines from a smaller number of dots in millimeter-size etched mesa structures (22, 23), as well as the cathodoluminescence (CL) work presented here.

In this work, CL is used to obtain spectral decomposition of the broader PL QD ensemble into lines narrower than 1 meV. This spectroscopic resolution is a direct consequence of the reduced dimensionality of these structures and permits, in some cases, direct imaging of single QDs.

Making QDs in the visible range by molecular beam epitaxy (MBE) has potentially interesting technological applications. The reduced density of states associated with 0D confinement could be exploited in the population inversion required for lasing, as long as the interlevel spacings are sufficiently large (24). A QD semiconductor laser could lead to spectral gain curves with a higher maximum (2). The production of QDs that emit visible light demonstrates that this technological advance can be expanded to optical devices in a wide range of wavelength and that the spontaneous coherent island formation has general applicability.

Samples in this study were prepared by MBE growth. Substrates were (001) semi-insulating GaAs. Temperatures were determined with a calibrated pyrometer. An As_4 partial pressure of 9×10^{-6} torr was maintained throughout the growth. After oxide desorption, a GaAs undoped buffer layer of 0.5 to 1 μm was grown at 600°C. The cladding layer was then grown, at 650°C, with either AlAs or AlGaAs. The strained islands were InAs or AlInAs. After cooling the samples to 530°C, In or In and Al molecular beams were pulsed in short cycles at low growth rates, resulting in the deposition of small amounts of InAs ($\ll 0.1$ monolayers per cycle). This was done until the transition from 2D growth to 3D growth was observed in the reflected high-energy electron diffraction (RHEED) pattern (17). The Al or the Al and Ga shutters were then simultaneously opened, and growth was continued in order to cover the strained islands with AlAs or AlGaAs, while the temperature was ramped back to 650°C. A 10-nm GaAs cap was grown as the last layer to protect the AlGaAs or AlAs from oxidation.

Island sizes, concentrations, and distribution, as well as the wetting layer and island thicknesses, were determined with plan view and cross-sectional transmission electron microscopy (TEM). A JEOL 200 FX operated at 200 KeV was used. Conventional polishing and ion milling was used to thin cross-section samples, and dimpling and chemical etching to perforation were used for the plan view samples.

The CL spectra and images were obtained with a JEOL 120 scanning TEM

R. Leon and S. Fafard, Center for Quantized Electronic Structures (QUEST), University of California, Santa Barbara, CA, 93106, USA.

P. M. Petroff, Center for Quantized Electronic Structures (QUEST), Materials Department, and Electrical and Computer Engineering Department, University of California, Santa Barbara, CA, 93106, USA.

D. Leonard, Center for Quantized Electronic Structures (QUEST) and Materials Department, University of California, Santa Barbara, CA, 93106, USA.

*To whom correspondence should be addressed at the Department of Electronic Materials Engineering, Research School of Physical Sciences and Engineering, Australian National University, Canberra, ACT 0200, Australia.

†Present address: Institute for Microstructural Sciences, National Research Council, Ottawa, Canada, K1A 0R6.

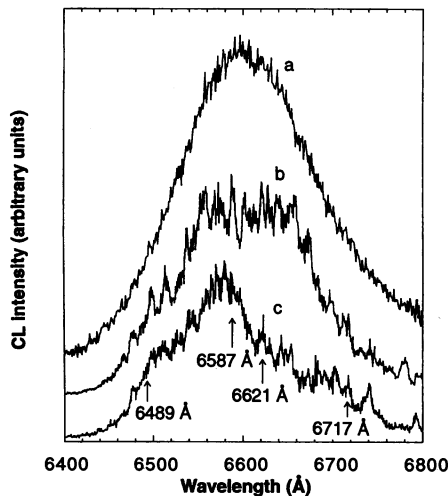


Fig. 1. Low-temperature (10 K) CL spectra for QD ensembles of different sizes in the InAlAs-AIGaAs sample. These were obtained at low magnification with (spectrum a) a defocused electron beam on a thick sample and (spectra b and c) a focused electron beam on a thin sample. Spectra b and c were obtained from different areas of the sample. A 120-keV, 82-mA electron beam was used.

instrument operated at 120 KeV and adapted with an ellipsoidal mirror. The CL signal was resolved by a 0.85-m double spectrometer and detected with a photomultiplier tube. Thinned samples were mounted on a low-temperature stage equipped with a thermocouple, and a constant-transfer liquid-He line was used to maintain the sample temperature around 10 K. This system simultaneously allowed observation of the QDs in the scanning transmission mode and CL analysis of the same area.

Low-temperature CL measurements are shown in Fig. 1 for one of the $\text{In}_{0.55}\text{Al}_{0.45}\text{As}-\text{Al}_{0.35}\text{Ga}_{0.65}\text{As}$ samples that showed a strong visible QD ensemble luminescence signal peaking at 660 nm (red). These nominal ternary compositions were chosen so as to obtain large direct band gaps for the AlGaAs layers and to raise the band gap in the QD layers without undergoing the indirect transition for InAlAs. Avoiding the presence of a very thick wetting layer under the islands was also a consideration. Visible luminescence has also been produced from different combinations in the $\text{In}_x\text{Al}_{(1-x)}\text{As}-\text{Al}_y\text{Ga}_{(1-y)}\text{As}$ system (25).

Figure 1 shows the CL spectra of this sample taken under different conditions. The luminescence of a thick sample measured using a defocused electron beam (Fig. 1, spectrum a) had the same broad Gaussian shape obtained in the PL measurements (25). In both CL and PL, the AlGaAs peak at 623 nm is seen. This broad peak [full width at half maximum (FWHM), 46 meV] corresponds to the exci-

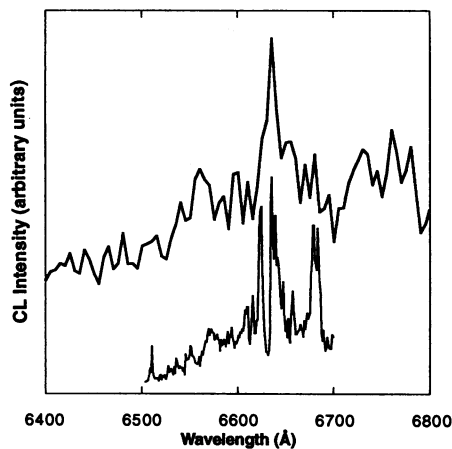


Fig. 2. Low- and high-resolution CL spectra from the same area obtained with a very thin sample and a small condenser aperture. The spectrum is no longer Gaussian because of the small number of QDs probed. This spectrum corresponds to the excitation of only a few tens of dots.

tation of a large number of dots, and it is attributed to slight variations in the OD confining potentials caused mostly by size dissimilarities. Spike-like features appear over the broader background in spectrum a of Fig. 1 because of the excitation of a smaller number (26) of dots in CL than in PL, even with a defocused electron beam.

The CL measurements were done with electron probes of successively smaller diameters (27). Also, a thin sample (~ 1500 Å, which is transparent to the electron beam) was used to minimize multiple dot excitation caused by backscattered electrons and x-rays produced in the substrate by the electron beam. The resulting spectra (Fig. 1, spectra b and c) display very sharp peaks, a fraction of a millielectron volt in width, originating from either individual dots or a few dots with equal or almost equal dimensions. These spikes are reproducible and are therefore not simply noise. These spectra (Fig. 1, spectra b and c) show different sets of peaks; while the sharpness of the features is maintained, the peaks have different intensities because they were taken from different areas in the sample, thus probing different dot ensembles.

The peak width determined from our resolution in the CL experiment is 0.6 meV, slightly larger (28) than the results obtained with lower temperature (2 K) PL experiments of etched mesas in the same sample, which gave a peak width as small as 0.4 meV (22). Considering the large size of the ensembles in the latter experiment and the possibility of broadening from several dots with very similar sizes, this remains an upper limit for the individual dot line width. The narrowness of these lines is a direct consequence of the OD quantum confined states,

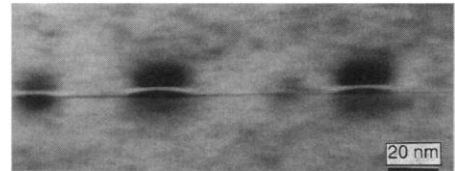


Fig. 3. Dark-field cross-sectional TEM micrograph of InAs-AIGaAs QDs imaged with (200) as the operating reflection. The wetting layer visible in this micrograph is always observed in these strained islands. Also apparent here is the spatial nonuniformity of the strain distribution, both in the islands and in the cladding material.

where the density of states approaches that represented by a Dirac delta function.

Transitions producing the CL described here arise most likely from the ground states of electrons and holes in the individual QDs. The possibility that some of these peaks might arise from excited quantum states is small. Calculations give an estimated value of the interlevel spacing of ~ 30 meV. Measured (19) interlevel spacings in a system with similar confinement potential were found to be >25 to 30 meV. Simultaneous radiative recombination from excited states and the ground states would result in a non-Gaussian (29) shape of the PL peak for the dot ensemble. Our measurements show this peak to be Gaussian with a 46-meV FWHM.

The excitation area is larger than the beam diameter (~ 100 Å) because carriers thus generated diffuse to nearby dots. The excitation diameter estimated from the spectra obtained with the focused-beam condition is ~ 0.5 μm . Planar dot density in this sample has been measured with plan view TEM (25), so it is estimated that individual peaks can be resolved from ~ 50 dots (30).

The PL and CL peaks are Gaussian for an infinite (or very large) dot ensemble. Measurements of large number of dot diameters from both atomic force microscopy (31) and TEM measurements (25) show that the size distribution for these islands is also Gaussian. The luminescence signal exhibits larger fluctuations from this Gaussian envelope when the number of dots probed gets smaller. The spectrum (Fig. 2) shows a non-Gaussian shape, resulting from the statistics of a small number of dots. The small signal collected from this type of measurement decreases the spectroscopic resolution of the experiment because larger slit widths are required.

The luminescence producing the ultra-sharp peaks in spectra b and c of Fig. 1 is spatially localized, corresponding to the QDs that give the characteristic strain contrast seen in the TEM micrograph (Fig. 3). Imaging the CL intensity is achieved by choosing

a few prominent peaks in the spectrum, setting the monochromator at these distinct energies, and scanning the variation in intensity across the same region of the sample.

Figure 4 shows four CL images for the same portion of the sample where the intensities for different wavelengths of visible photons were collected. The different luminescence patterns emerging indicate that the sharp lines originate from different regions in the sample. Imaging at selected wavelengths enables resolution of the luminescence from individual QDs. This is only possible because there is a distribution in sizes with a corresponding distribution in luminescence energies; if all of the dots in the sample were luminescing at a given energy, it would not be possible to resolve them because the average dot spacing is smaller than the CL resolution ($\sim 0.5 \mu\text{m}$). The same technique can be used with line scans, and this facilitates the estimation of the resolution of this system. Measurements from line scans also show that it is possible to resolve the luminescence from QDs that are $0.5 \mu\text{m}$ apart emitting at exactly the same wavelength.

A straightforward statistical analysis with the use of Figs. 1 and 4 reveals that at least two of the four scans show the luminescence from individual QDs. This was done by using the fact that the peak ensemble for the sample in question can be fitted with a normal or Gaussian distribu-

tion. The spectral resolution for the image acquisition part of the experiment was $\delta\lambda = 10 \text{ \AA}$. It can then be determined, with knowledge of the areal density of the dots in the sample and the broadening of the Gaussian distribution [best determined with PL measurements (25) and the CL measurements for the large excitation volume conditions seen in spectrum a of Fig. 1], that the probability of finding more than one dot within a spot $0.5 \mu\text{m}$ in diameter is negligible in the images obtained for $\lambda = 6717$ and 6498 \AA . For the images obtained with $\lambda = 6587$ and 6621 \AA , each square measuring $0.5 \mu\text{m}$ on a side might contain two to three dots emitting at the energy interval chosen. This situation is reflected at the higher resolution seen in the first and last image, and it is a consequence of scanning with selected wavelength near the tail ends of the distribution.

Future challenges will include attempts to make ordered 2D and 3D arrays of these structures. Ordering in the growth direction might be easily achieved if advantage is taken of the far-reaching strain field. Ordering along the plane of the island formation presents greater difficulties, even though some progress has been made in this regard with different substrate orientations (32). Other areas of interest will involve the incorporation of these structures in devices like 0D resonant tunnel diodes and in semiconductor QD lasers.

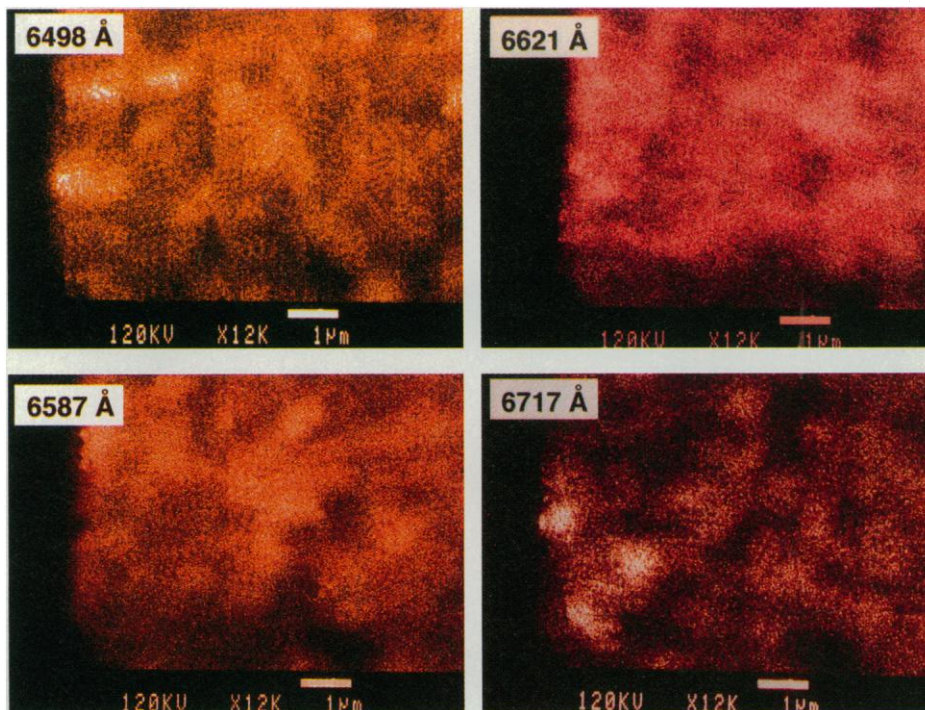


Fig. 4. CL images of the same section of a sample at four of the wavelengths that produce the sharp peaks shown in spectra c in Fig. 1. The brighter areas correspond to higher intensities of luminescence at the chosen wavelength.

REFERENCES AND NOTES

- For a typical III-V semiconductor, 3D confinement effects will start to be observable for a volume under $5 \times 10^{-18} \text{ cm}^3$ or $< 50,000$ atoms.
- C. Weisbuch and B. Vinter, *Quantum Semiconductor Structures* (Academic Press, New York, 1991), and references therein.
- F. C. Frank and J. H. van der Merwe, *Proc. R. Soc. London Ser. A* **198**, 205 (1949).
- M. Volmer and A. Weber, *Z. Phys. Chem.* **119**, 277 (1926).
- I. N. Stranski and Von L. Krastanow, *Akad. Wiss. Lit. Mainz Math. Naturwiss. Kl.* **146**, 797 (1939).
- D. J. Eaglesham and M. Cerullo, *Phys. Rev. Lett.* **64**, 1943 (1990).
- B. Elman *et al.*, *Appl. Phys. Lett.* **55**, 1659 (1989).
- S. Z. Chang, T. C. Chang, S. C. Lee, *J. Appl. Phys.* **73**, 4916 (1993).
- C. W. Snyder, J. F. Mansfield, B. G. Orr, *Phys. Rev. B* **46**, 9551 (1992).
- C. W. Snyder, B. G. Orr, D. Kessler, L. M. Sander, *Phys. Rev. Lett.* **66**, 3032 (1991).
- F. Houzay, C. Guille, J. M. Moison, P. Henoc, F. Barthe, *J. Cryst. Growth* **81**, 67 (1987).
- J. M. Gerard, *Appl. Phys. Lett.* **61**, 2096 (1992).
- O. Brandt *et al.*, *Phys. Rev. B* **44**, 8043 (1991).
- L. Goldstein, F. Glas, J. Y. Marzin, M. N. Charasse, G. Le Roux, *Appl. Phys. Lett.* **47**, 1099 (1985).
- S. Guha, A. Madhukar, K. C. Rajkumar, *ibid.* **57**, 2110 (1990).
- F. K. LeCoq, M. C. Reuter, J. Tersoff, M. Hammar, R. M. Tromp, *Phys. Rev. Lett.* **73**, 300 (1994).
- D. Leonard, M. Krishnamurthy, C. M. Reaves, S. P. Denbaars, P. M. Petroff, *Appl. Phys. Lett.* **63**, 3203 (1993).
- D. Leonard, M. Krishnamurthy, S. Fafard, J. L. Merz, P. M. Petroff, *J. Vac. Sci. Technol. B* **12**, 1063 (1994).
- S. Fafard, D. Leonard, J. L. Merz, P. M. Petroff, *Appl. Phys. Lett.* **65**, 1388 (1994).
- Magnetocapacitance studies show evidence for a peaked density of states.
- H. Drexler, D. Leonard, W. Hansen, J. P. Kotthaus, P. M. Petroff, *Phys. Rev. Lett.* **73**, 2252 (1994).
- S. Fafard, R. Leon, D. Leonard, J. L. Merz, P. M. Petroff, *Phys. Rev. B* **50**, 8086 (1994).
- J. Y. Marzin, J. M. Gerard, A. Izrael, D. Barrier, G. Bastard, *Phys. Rev. Lett.* **73**, 716 (1994).
- E. Kapon, D. M. Hwang, M. Walther, R. Bhat, N. G. Stoffel, *Surf. Sci.* **267**, 593 (1992).
- R. Leon, S. Fafard, D. Leonard, J. Merz, P. M. Petroff, in preparation.
- The spectra are similar to those in the experiment described in (20), where large mesas are delineated, corresponding to the excitation of ~ 4000 dots.
- The corresponding electron beam diameter can be either 500 \AA or 50 to 100 \AA , depending on the condenser aperture used.
- Thermal broadening (0.9 meV for the CL measurements) might also have to be considered here.
- Simultaneous emission from two eigenstates 30 meV apart would either give a bimodal distribution or add a "shoulder" to the Gaussian peak, making it asymmetric.
- The best estimates of the CL spatial resolution in these experiments were done taking the narrower FWHM of intensity-variation peaks in line scans obtained for a fixed wavelength.
- D. Leonard, K. Pond, P. M. Petroff, *Phys. Rev. B* **50**, 11687 (1994).
- R. Notzel, J. Temmyo, T. Tamamura, *Nature* **369**, 131 (1994).
- The authors would like to thank M. Krishnamurthy for initiating this work at the University of California, Santa Barbara, T. Tran and J. English for technical assistance, and A. Gossard for critical reading of the manuscript. This research was supported by National Science Foundation Science and Technology Center QUEST (DMR #91-20007) and the Air Force Office of Scientific Research (F9620-98-J0214). S.F. would like to acknowledge the National Science and Engineering Research Council of Canada for financial support.

16 August 1994; accepted 5 January 1995